

# On the capability of deep level transient spectroscopy for characterizing multi-crystalline silicon

T. Mchedlidze, M. Nacke, E. Hieckmann, and J. Weber  
*Technische Universität Dresden, 01062 Dresden, Germany*

(Received 16 July 2013; accepted 16 September 2013; published online 2 January 2014)

The suitability of the deep level transient spectroscopy (DLTS) technique in exploring locations with high and degraded carrier lifetimes containing grain-boundaries (GBs) in multicrystalline silicon (mc-Si) wafers was studied. The types and locations of GBs were determined in mc-Si samples by electron backscatter diffraction. Mesa-type Schottky diodes were prepared at (along) GBs and at reference, GB-free locations. Detected DLTS signals varied strongly along the same GB. Experiments with dislocation networks, model structures for GBs, showed that GB-related traps may be explored only using special arrangement of a GB and the diode contacts. Iron-related carrier traps were detected in locations with degraded carrier lifetimes. Densities of the traps for near-GB and for GB free locations were compared to the lifetime measurement results. © 2014 AIP Publishing LLC. [<http://dx.doi.org/10.1063/1.4837997>]

## I. INTRODUCTION

The growing demand for cheaper and better quality multicrystalline silicon (mc-Si) for photovoltaic (PV) industry requires application of advanced methods for in-depth quantitative characterization of its properties. The specific difficulty related to mc-Si material lies in the broad variety of point-like and extended defects, which are incorporated during the solar cell fabrication processes.<sup>1</sup> Widely used methods for PV material characterization are based on carrier lifetime measurements.<sup>2</sup> The results of such measurements could be directly linked to the expected efficiency of the solar-cells.<sup>2</sup> These techniques allow quasi-in-line control of the PV-material quality during production of solar-cells. However, in most cases these methods are unable to associate the degradation of carrier lifetime with a specific defect and, moreover, are not able to distinguish between the many defects and carrier traps existing in mc-Si. More defect-specific methods, based on the luminescence were also widely investigated and applied.<sup>3–5</sup> However, defect-luminescence based methods are mostly qualitative and require careful consideration of optical inhomogeneities and surface conditions of the mc-Si material.<sup>6</sup>

A quantitative method suitable for analyses of defect related traps in semiconductors is the deep level transient spectroscopy (DLTS).<sup>7</sup> The method determines trap densities, their energy level positions in the band-gap, and carrier capture cross-sections. In addition, it gives a possibility to differentiate point-like defects from extended ones,<sup>8</sup> allows determining the charge state of a trap,<sup>9</sup> and among others, determines a profile of a trap density close to the sample surface.<sup>7</sup> The method was broadly applied for investigating the properties of numerous defects in crystalline Si, in thin-film Si solar cells<sup>10</sup> and traps in the pn-junctions of the crystalline solar cells.<sup>11</sup> Recent studies on defect states related to dislocation networks<sup>12–14</sup> indicate possible ways to apply the DLTS method for exploring properties of grain-boundaries (GBs) in mc-Si. Several previously reported attempts to measure GB-related DLTS signals in mc-Si were

controversial.<sup>15–20</sup> Namely, the results strongly depended on the arrangement of the electrical contacts fabricated for the measurements<sup>18–20</sup> and on the presence of contaminant atoms at/near to GBs.<sup>15–17</sup> Differently from the results obtained for the dislocation networks,<sup>12–14</sup> no clear relations of the detected signals with the structural properties of GBs in mc-Si were proposed.

In the present study, we explored the capability of DLTS for detection of defect states related to GBs in mc-Si. The results obtained for mc-Si were compared to those for dislocation networks in directly bonded silicon wafers. Besides that, the DLTS signals from locations with degraded carrier lifetimes containing GBs and those for GB-free, reference locations were also investigated.

## II. SAMPLES AND EXPERIMENTAL

Silicon samples used in this study were prepared from a mc-Si ingot grown by the vertical gradient freeze method<sup>1</sup> (VGF) at SCHOTT Solar Wafer GmbH. Resistivity of the B-doped wafer cut-out from edge brick of the mc-Si ingot was  $\sim 1 \Omega \text{ cm}$ . Measurements of effective carrier lifetime, performed at Freiberg Instruments GmbH, indicated strong degradation of the lifetime close to the edge of the wafer. The averaged lifetime gradient for the near-to-edge locations of the sample will be presented later. The sample for the study was cut from the wafer in such a way that it contained regions with high and with degraded carrier lifetimes. The image of the sample after mechanical polishing and etching is presented in Fig. 1(a). After cleaning and etch-off of native oxide, 50 nm thick Al film was deposited on the surface of the sample and the locations planned for the DLTS measurements were covered with protective varnish (see Fig. 1(b)). The varnish hardened at room temperature and subsequently the sample was etched in  $\text{HF}+\text{HNO}_3$  (1:5) solution to remove the Al film and Si from the unprotected locations to the depth of  $\sim 50 \mu\text{m}$ . Further, the varnish was removed by special thinner and the sample was rinsed in acetone to open the electrical contacts to the mesa-type Schottky diodes. The

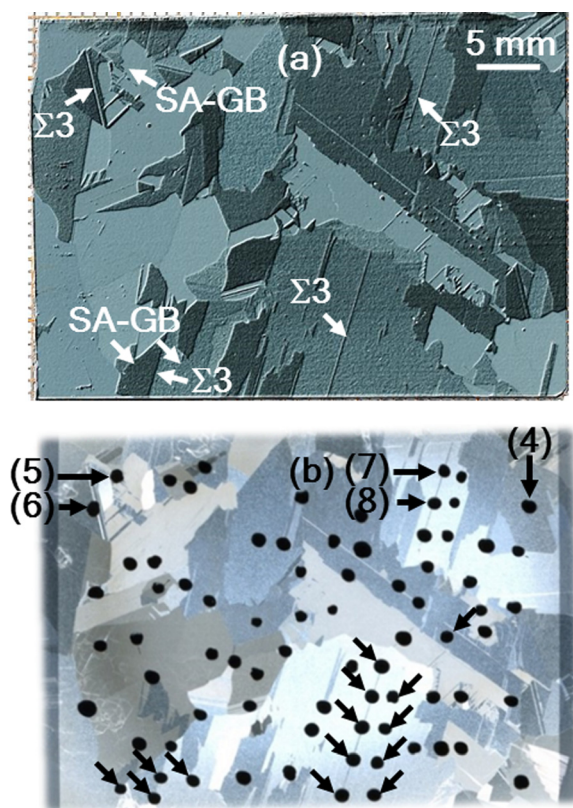


FIG. 1. Images of the mc-Si sample after polishing and etching (a) and after deposition of Al film and varnish (b). White arrows in (a) indicate the GBs with the type determined by EBSD. Black arrows in (b) indicate locations where DLTS measurements were performed.

sample was cut into smaller pieces, i.e.,  $\sim 10 \times 5 \text{ mm}^2$  in size, appropriate for mounting on the DLTS sample holder. Ohmic contacts were formed by rubbing-in InGa eutectic solution to the back surface of the samples. Areas of the mesa-diodes were estimated from their images.

Wafers from mc-Si ingots are usually cut perpendicular to the solidification direction, therefore GBs are inclined into wafer surfaces at angles close to  $90^\circ$ .<sup>1</sup> The type of a GB (misorientation angle and axis) was determined from the orientation of the adjacent grains by electron backscatter diffraction (EBSD, see, e.g., Ref. 21). Measurements were carried out by a Zeiss Ultra 55 FEG-SEM equipped with a Nordlys EBSD detector and HKL Channel5 software at 20 kV and probe current of 10 nA, respectively. The mapping step size was in the range of  $2\text{--}20 \mu\text{m}$  according to the mean grain size. Boundaries with misorientation angle (MOA)  $< 15^\circ$  were classified as small-angle (SA-) GBs, those with MOA  $> 15^\circ$  as large angle (LA-) GBs. The latter can be separated on GBs that can be described by the Coincident Site Lattice Theory ( $\Sigma$  GBs) and on random GBs. In this study we will present data related to  $\Sigma 3$ , SA-GB and to reference locations, not containing GBs. The investigated locations are indicated in Fig. 1(b) by arrows and the types of the selected GBs are shown in Fig. 1(a).

Dislocation networks (DNs) formed during direct bonding of two silicon wafers represent structures closely resembling GBs in mc-Si.<sup>22</sup> Two boron doped Cz-Si wafers with initial resistivity  $\sim 10 \Omega \text{ cm}$  were used for the direct wafer

bonding in the hydrophilic processes by SOITEC. The buried oxide layer remaining at the interface after the bonding was dissolved by subsequent annealing in vacuum at high temperatures. Details of the bonding procedure can be found elsewhere.<sup>23</sup> After the fabrication procedure, the DN was located at a depth of  $\sim 160 \text{ nm}$  from the sample surface and was lying parallel to it. The structure of the DN can be characterized by a tilt angle of  $< 0.5^\circ$  and by a twist angle of  $3.5^\circ$  between orientations of the wafers used in the bonding process.<sup>24</sup> Our EBSD measurements confirmed these values. The homogeneity of a DN structure over the whole bonded wafer surface was verified in the previous investigations (see Ref. 24 and references therein).

The structures sketched in Fig. 2 were fabricated from the samples containing DN using procedures similar to those described above for the mc-Si samples. Three distinct geometries of DN in the space charge region (SCR) of the Schottky diode were modeled. For the structure in Fig. 2(1), the DN plane was parallel to the plane of the Schottky diode. For the structure in Fig. 2(2), the DN plane was inclined into the Schottky diode structure, while a substantial part of it was still parallel to the contact. In the case shown in Fig. 2(3), the DN plane was lying mainly perpendicular to the plane of the Schottky contact. For standard DLTS measurements, the metal layer for the Schottky contact is deposited on the mc-Si wafer surface. Thus, the geometry in Fig. 2(3) for the DN most closely resembles the case occurring during DLTS measurements of locations with GBs in mc-Si samples.<sup>18,19</sup>

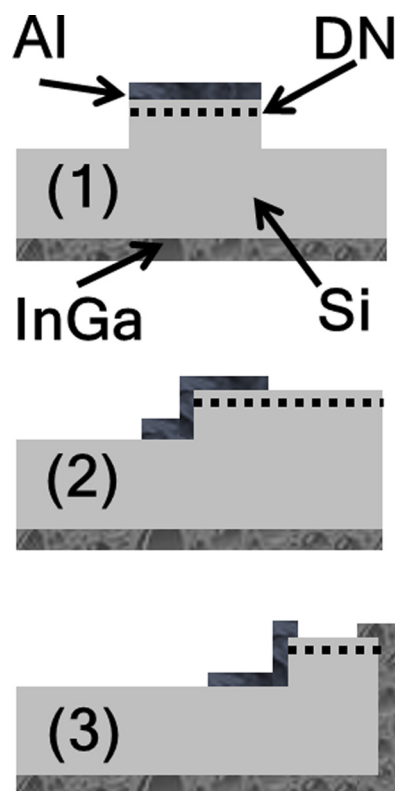


FIG. 2. Sketches of the samples containing DN and various configurations of Schottky and Ohmic contacts. The images are not scaled to the real dimensions.

DLTS measurements were performed by means of a standard lock-in system working at the capacitance testing frequency of 1 MHz. Principles of the method and the system were previously described.<sup>25</sup> A sample was mounted in a He-dewar and its temperature was controlled in the range 35–300 K.

### III. RESULTS AND DISCUSSION

#### A. DLTS spectra from locations with non-degraded lifetime

For the possible detection of GB-related traps, we selected locations with the largest effective lifetimes in the mc-Si sample containing  $\Sigma 3$ -GB (6, 7, 8) and SA-GB (5). A location inside the ingrain material (4) was selected as a reference. These locations are indicated by numbered arrows in Fig. 1(b). The DLTS spectra obtained from the mesa-diodes are presented in Fig. 3(a).

Note, that the signals from GB-containing locations (5–8) had mostly negative sign. Previously, negative signals were already attributed to GBs.<sup>18,19</sup> Possible origin of the

negative sign for signals was also proposed and discussed (see Ref. 19 and references therein). However, observed drastic differences in the shape and intensity between the spectra (6–8) originating from the different locations along the same  $\Sigma 3$ -type GBs question attribution of the spectra to the same GB structure. Carrier lifetime measurements also have not indicated any significant differences between the locations (6–8). We decided to check an influence of the diode contact arrangement on the results of the measurements.

To explore possible influence of an arrangement of the contacts on the DLTS signals from GBs, we measured DLTS spectra from the three structures containing DNs as described in Fig. 2. The resulting spectra are presented in Fig. 3(b). The spectrum detected from the structure (1) closely resembles those reported previously for the similar DNs.<sup>12–14</sup> The low and the high temperature peaks were ascribed to deep and shallow traps associated with the DNs. Our study showed very close similarities of the detected signals to those reported previously.<sup>12,13</sup> Therefore, we will not reproduce the results here, but refer the reader to the publications, which give details of the signals and their attribution to the DN structures.<sup>12–14</sup>

For the structure sketched in Fig. 2(2), the DLTS spectrum weakly resembled that from the structure (1). The peaks at low and high temperatures were also present, but their amplitudes were suppressed and shapes of the peaks were distorted. Moreover, the negative component of the signal appeared in the spectrum. For structures like the one shown in Fig. 2(3), the intensities of the DLTS signals were even smaller and the spectrum was strongly influenced by the detailed arrangement of the electrical contacts.

Two reasons could be proposed for the explanation of the dependence of the DN-related DLTS signal on the contact geometry. First, the amount of DN traps in the SCR of the Schottky diode strongly decreases with increase in the inclination angle of the DN plane into the plane of the contact. Second, trapped carriers are mobile along the DN<sup>12–14,22</sup> and escape the SCR along the DN plane under action of the reverse bias before they could be thermally excited and contribute to the DLTS signal. Since during the measurements of mc-Si samples the contact arrangement resembled that sketched in Fig. 2(3), with high probability, we can suppose that the detected negative signals were not related to GB traps.

The origin of the detected negative signals in the spectra (5–8) and those reported previously<sup>18,19</sup> requires further investigations. The difficulty in such a study is, however, related to a poor repeatability of the spectra, i.e., their dependence on distinct location and on the contact arrangement. Interestingly, the peaks like present in spectra (5) and (6) resemble those detected from dislocations and/or from oxide precipitates in Si,<sup>26,27</sup> but the former have negative sign. We speculate that the signals originate from extended defects located close to a GB and the negative sign corresponds to an exchange of carriers between the defects and the GB after termination of the filling pulse. Such a mechanism is similar to those suggested in the previous publications,<sup>15,17</sup> but besides carrier exchange inside the GB should include the exchange between GB and the surrounding traps.

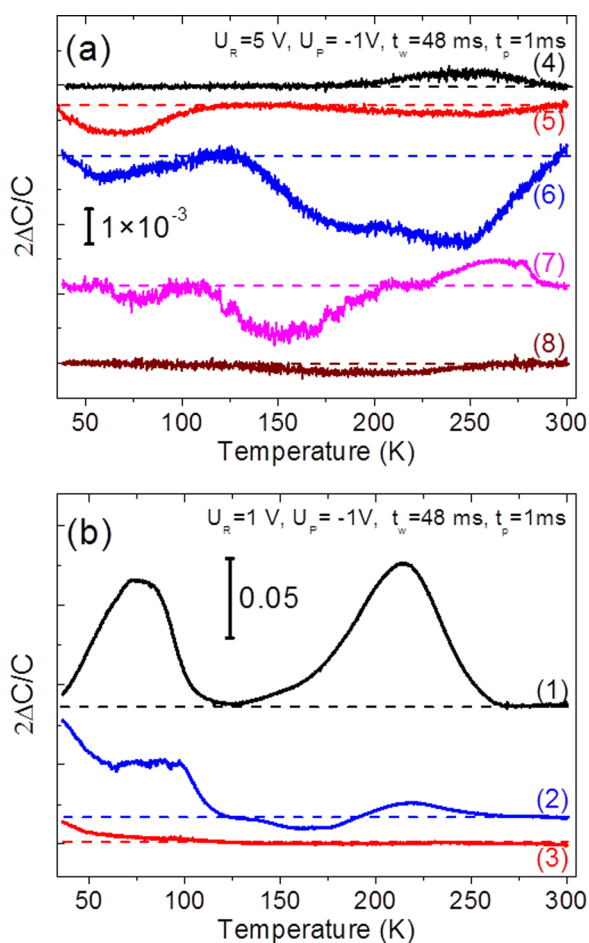


FIG. 3. DLTS signals detected from the locations with large carrier lifetime in mc-Si sample (a) and from the DN structures (b). Curve numbers in (a) correspond to the numbered arrows in Fig. 1(b) and in (b) to the structure numbers in Fig. 2. Measurement conditions indicated in the figures correspond consequently to the reverse bias ( $U_R$ ), pulse bias ( $U_P$ ), sampling time ( $t_w$ ), pulse duration ( $t_p$ ) during the measurements. The spectra are shifted vertically for ease of viewing. Dotted lines present the null signal level for each spectrum.



A weak DLTS signal in high temperature range was detected from the reference ingrain location (see curve (4) in Fig. 3(a)). The energy level position in the bandgap at  $E_V + 0.44$  eV and the effective carrier capture cross-section value  $\sigma = 2.2 \times 10^{-15}$  cm<sup>2</sup> were determined for the related trap. The signal intensity increased linearly with the logarithm of the filling pulse duration pointing to extended character of the defects.<sup>8</sup> Based on these characteristics, the signal was attributed to oxide precipitates.<sup>27</sup>

The presented results suggest that the study of GB-related traps in mc-Si cannot be performed without specially fabricated samples, where the GB is positioned parallel to the Schottky contact inside the SCR of a mesa-diode, i.e., in compliance to the sketch presented in Fig. 2(1). Such samples with well-defined GB structure could be prepared from bicrystals, from specially cut mc-Si ingots or by direct wafer bonding. Therefore, the results reported in Refs. 15–21, for the traps attributed to various GBs should be verified using the specially prepared samples and the correct contact arrangement.

## B. DLTS spectra from locations with degraded carrier lifetimes

Degradation of carrier lifetime close to the walls of the mc-Si ingot was attributed to the diffusion of Fe atoms from the material of crucible walls.<sup>28</sup> In the present work, we explored a distribution of iron-boron (FeB) pairs in the locations with degraded lifetime and the influence of GBs on the distribution. The studied locations of diodes containing  $\Sigma$ 3-GBs, SA-GBs, and the reference locations are indicated in the lower half of the image in Fig. 1(b) by arrows. The effective carrier lifetime gradually increased in the sample from the edge corresponding to the bottom of the image in the vertical direction and saturated at the value of  $\sim 2$   $\mu$ s at the distance  $\sim 15$  mm from the top. The spectra from the diodes with GBs were similar to those presented in Fig. 3(a), however, in addition positive signals from FeB traps were detected at  $\sim 50$  K. The FeB trap related signal and a weak signal at  $\sim 105$  K, labeled H105, were detected at the reference locations. Examples of signals detected at a distance of  $d \approx 7$  mm from the lower edge of the sample (see Fig. 1) are presented in Fig. 4. Attribution of the traps to FeB pairs was confirmed by comparison of their parameters with those presented in the previous publications.<sup>29</sup> The energy level position in the bandgap at  $E_V + 0.2$  eV and the effective carrier capture cross-section value  $\sigma = 2 \times 10^{-15}$  cm<sup>2</sup> were determined for the H105 trap from the Arrhenius plot. The H105 signal was detected only for the reference locations and its intensity was at the level of  $\sim 0.1$  of that for FeB.

In Fig. 5, the FeB trap density for each diode and average effective lifetimes are presented for various distances from the wafer edge. In the graph, the distance  $d$  was estimated from the lower edge of the sample (see Fig. 1). As seen from the figure, the dependencies of FeB trap density from  $d$  look similar for the reference locations and for those containing GBs. However, the values of the densities are suppressed for  $\Sigma$ 3-GB containing locations and even stronger suppressed for the locations containing SA-GBs. This

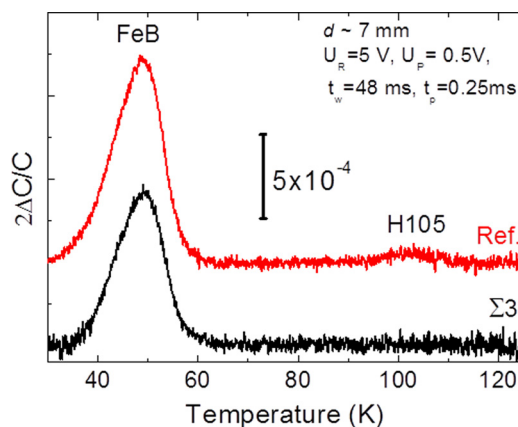


FIG. 4. DLTS signals detected from the mc-Si sample at the distance of  $\sim 7$  mm from the lower edge (see Fig. 1) at the  $\Sigma$ 3-GB and at the reference location. The spectra are shifted vertically for ease of viewing. For the suitable signal to noise ratio the measurements were performed at a very low temperature ramp rate ( $\leq 2$  K/min).

may be related to the ability of GBs to getter impurity atoms, i.e., iron atoms in Si.<sup>21</sup> Indeed, formation of FeB traps may be suppressed if Fe atoms will be gettered to nearby GBs. This supposition is also supported by the fact that FeB signals close to SA-GBs were even less intensive than those close to  $\Sigma$ 3-GBs, since the structure of SA-GB is much more defective and could accommodate more impurity atoms.<sup>21</sup>

Interestingly, FeB trap density did not increase gradually to the edge of the sample, as could be expected from the lifetime data. It should be noted that the lifetime measurements were performed for the thin wafer, therefore only effective carrier lifetime was estimated;<sup>30</sup> still the gradient of the measured lifetime should reflect the change in the carrier trap density in the material. From the comparison between the FeB trap density distribution and the lifetime data, it can be deduced that FeB pairs do not represent the main lifetime killers close to the wafer edge.

Origin of the H105 trap remains to be clarified. Since its density correlates with that for FeB traps, it might be valid to assume that the trap also contained Fe atoms. From the known Fe-related traps, the parameters best match those

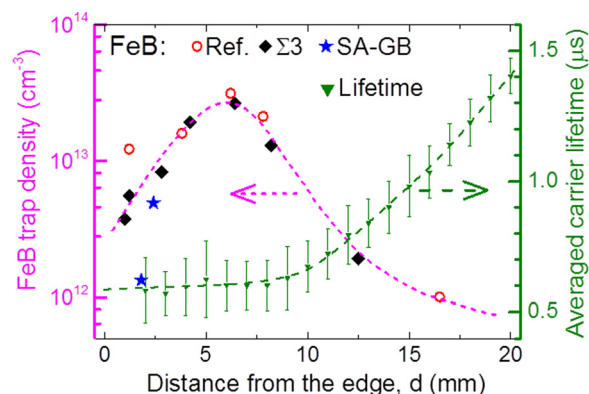


FIG. 5. Dependencies of the FeB trap density and of the averaged effective carrier lifetime from the distance from the lower sample edge (see Fig. 1). Curves are presented for ease of viewing. Attributions of the data to the axes are shown by the arrows. Each FeB trap density value corresponds to the location indicated by the arrow in Fig. 1(b).

assigned to the  $\text{Fe}_2\text{V}_2$  complex in iron-contaminated Si sample subjected to electron irradiation and subsequent annealing.<sup>31</sup> Since the presence of vacancy complexes in the near-to-wall region of the casted mc-Si ingot was not reported previously, the coincidence of the parameters may be accidental. On the other hand, the assignment<sup>31</sup> was proposed based only on the analogy between Fe- and Sn-related trap formation and should be verified in the future. The H105 traps are also suppressed near to GBs, thus probably GBs present sinks for the components of the related complex.

#### IV. SUMMARY

Deep level transient spectroscopy was applied for characterization of samples prepared from PV-grade mc-Si wafers. Attempts to detect traps related to GBs were not successful. The detected DLTS signals resembled those from dislocations and/or from oxide precipitates but had negative sign. Analyses of the results obtained using bonded samples containing dislocation networks, suggested that for the proper detection of GB-related traps it is essential to use a special geometry of the contacts: the GB under investigation should be located parallel to the plane of a Schottky diode, inside the space charge region. Since most GBs in standard mc-Si wafers are inclined to the surface at an angle close to 90°, detection of the GB-related traps for mc-Si wafers present substantial difficulty. In the opinion of the authors, characterization of the traps related to the GBs of prevalent types, i.e.,  $\Sigma 3$ ,  $\Sigma 9$ ,  $\Sigma 27$ , etc., should be performed using specially prepared model structures. Once properties of the traps related to GBs with most abundant structures will be established, prediction of the material performance based on the structural analyses and relevant tailoring of the solar cell fabrication processes will become possible.

Investigations of locations near to the wall of mc-Si ingot showed that the lifetime degradation there could not be attributed solely to the presence of FeB traps. The maximum in the FeB trap density was detected for  $\sim 7$  mm distance from the ingot edge, while the measured effective lifetime values were gradually increasing from the edge. Near to GBs the density of the FeB traps was slightly suppressed, the effect was stronger for the SA-GB in comparison to  $\Sigma 3$ -GB. The effect was attributed to gettering of Fe atoms by GBs.

#### ACKNOWLEDGMENTS

The work was supported by the German Ministry for Education and Research under Contract 03SF0398K ( $x\mu$ -Material) in the framework of the Excellence Cluster Solar Valley Central Germany. We would like to thank O. Kononchuk (SOITEC) for providing the bonded Si samples and SCHOTT Solar for supplying mc-Si wafers. Special

thanks are due to K. Kurasch (TU Dresden) and Freiberg Instruments GmbH for conducting carrier lifetime measurements.

- <sup>1</sup>H. Rodriguez, I. Guerrero, W. Koch, A. L. Endrös, D. Franke, C. Häbeler, J. P. Kalejs, and H. J. Möller, *Handbook of Photovoltaic Science and Engineering*, edited by A. Luque and S. Hegedus (John Wiley & Sons, Ltd, West Sussex, United Kingdom, 2011), p. 218.
- <sup>2</sup>J. Isenberg, S. Riepe, S. W. Glunz, and W. Warta, *J. Appl. Phys.* **93**, 4268 (2003).
- <sup>3</sup>T. Trupke, R. A. Bardos, M. C. Schubert, and W. Warta, *Appl. Phys. Lett.* **89**, 044107 (2006).
- <sup>4</sup>B. Mitchell, J. W. Weber, D. Walter, D. Macdonald, and T. Trupke, *J. Appl. Phys.* **112**, 063116 (2012).
- <sup>5</sup>R. P. Schmid, D. Mankovics, T. Arguirov, M. Ratzke, T. Mchedlidze, and M. Kittler, *Phys. Status Solidi A* **208**, 888 (2011).
- <sup>6</sup>T. Mchedlidze, W. Seifert, M. Kittler, A. T. Blumenau, B. Birkmann, T. Mono, and M. Moeller, *J. Appl. Phys.* **111**, 073504 (2012).
- <sup>7</sup>D. V. Lang, *J. Appl. Phys.* **45**, 3023 (1974).
- <sup>8</sup>W. Schroeter, H. Hedemann, V. Kveder, and F. Riedel, *J. Phys.: Condens. Matter* **14**, 13047 (2002).
- <sup>9</sup>S. D. Ganichev, E. Ziemann, W. Prettl, I. N. Yassievich, A. A. Istratov, and E. R. Weber, *Phys. Rev. B* **61**, 10361 (2000).
- <sup>10</sup>T. Mchedlidze and M. Kittler, *J. Appl. Phys.* **111**, 053706 (2012).
- <sup>11</sup>T. Mchedlidze, L. Scheffler, J. Weber, M. Herms, J. Neusel, V. Osinniy, C. Möller, and K. Lauer, *Appl. Phys. Lett.* **103**, 013901 (2013).
- <sup>12</sup>M. Trushin, O. Vyvenko, T. Mchedlidze, O. Kononchuk, and M. Kittler, *Solid State Phenom.* **156–158**, 283 (2010).
- <sup>13</sup>M. Trushin, O. Vyvenko, T. Mchedlidze, M. Reiche, and M. Kittler, *Phys. Status Solidi C* **8**, 1371 (2011).
- <sup>14</sup>I. Kolevatov, M. Trushin, O. Vyvenko, M. Kittler, and O. Kononchuk, *Phys. Status Solidi C* **10**, 20 (2013).
- <sup>15</sup>A. Broniatowski, *Phys. Rev. B* **36**, 5895 (1987).
- <sup>16</sup>A. Bary, J. F. Hamet, A. Ihlal, J. L. Chermant, and G. Nouet, *J. Phys. Colloques* **49**, C5-665 (1988).
- <sup>17</sup>J. F. Hamet, R. Abdelaoui, and G. Nouet, *J. Appl. Phys.* **68**, 638 (1990).
- <sup>18</sup>D. P. Parton, T. Markvart, P. Ashburn, J. C. Carter, and L. Castaner, *Mater. Sci. Forum* **196–201**, 1903 (1995).
- <sup>19</sup>J. Chen, E. Cornagliotti, E. Hieckmann, S. Behrendt, J. Weber, E. Simoen, and J. Poortmans, *ECS Trans.* **33**, 71 (2011).
- <sup>20</sup>J. Chen, E. Cornagliotti, E. Simoen, E. Hieckmann, J. Weber, and J. Poortmans, *Phys. Status Solidi (RRL)* **5**, 277 (2011).
- <sup>21</sup>B. Chen, J. Chen, T. Sekiguchi, M. Saito, and K. Kimoto, *J. Appl. Phys.* **105**, 113502 (2009).
- <sup>22</sup>M. Kittler, X. Yu, T. Mchedlidze, T. Arguirov, O. F. Vyvenko, W. Seifert, M. Reiche, T. Wilhelm, M. Seibt, O. Voß, A. Wolff, and W. Fritzsche, *Small* **3**, 964 (2007).
- <sup>23</sup>O. Kononchuk, F. Boedt, and F. Allibert, *Solid State Phenom.* **131–133**, 113 (2008).
- <sup>24</sup>M. Reiche, *Mater. Sci. Forum* **590**, 57 (2008).
- <sup>25</sup>G. L. Miller, D. V. Lang, and L. C. Kimerling, *Annu. Rev. Mater. Sci.* **7**, 377 (1977).
- <sup>26</sup>V. V. Kveder, Yu. A. Osepyan, W. Schröter, and G. Zoth, *Phys. Status Solidi A* **72**, 701 (1982).
- <sup>27</sup>T. Mchedlidze, K. Matsumoto, and E. Asano, *Jpn. J. Appl. Phys., Part 1* **38**, 3426 (1999).
- <sup>28</sup>T. Buonassisi, A. A. Istratov, M. D. Pickett, J.-P. Rakotoniaina, O. Breitenstein, M. A. Marcus, S. M. Heald, and E. R. Weber, *J. Cryst. Growth* **287**, 402 (2006).
- <sup>29</sup>K. Wunstel and P. Wagner, *Appl. Phys. A* **27**, 207 (1982).
- <sup>30</sup>M. Turek, *J. Appl. Phys.* **111**, 123703 (2012).
- <sup>31</sup>P. Kaminski, R. Kozłowski, A. Jelenksi, T. Mchedlidze, and M. Suezawa, *Jpn. J. Appl. Phys., Part 1* **42**, 5415 (2003).